

Electrodeposition of nickel in the presence of Al^{3+} from sulfate baths

U.S. MOHANTY¹, B.C. TRIPATHY², P. SINGH³, S.C. DAS^{2,*} and V.N. MISRA²

¹Department of Materials Science and Engineering, National Cheng Kung University, Tainan, Taiwan, ROC 70101,

²Regional Research Laboratory (CSIR), Bhubaneswar, 751013, India

³Department of Chemistry, Murdoch University, Murdoch, WA 6150, Australia

(*author for correspondence, e-mail: drscdas@rrlbhu.res.in; phone: +91-674-2581635; fax: +91-674-2581637)

Received 31 March 2004; accepted 18 January 2005

Key words: aluminium, crystal orientations, current efficiency, deposit morphology, electrodeposition, kinetic parameters, nickel

Abstract

The effect of Al^{3+} on the cathodic current efficiency, deposit morphology, crystallographic orientations and polarisation behaviour of the cathode during electrodeposition of nickel from acidic sulfate solutions was investigated. Higher concentration of Al^{3+} ($> 10 \text{ mg dm}^{-3}$) significantly deteriorated the surface quality of the nickel deposit as well as the current efficiency. X-ray diffraction studies revealed that the (200) plane was the most preferred crystal plane and was not affected by the presence of varying concentration of Al^{3+} in the electrolytic bath. The presence of Al^{3+} caused polarisation of the cathode, which increased with increasing Al^{3+} concentration. The effect of Al^{3+} on the electrokinetic parameters: Tafel slope (b), transfer coefficient (α) and exchange current density (i_0) were also investigated.

1. Introduction

The leach liquors during the hydrometallurgical processing of nickel from raw materials are usually contaminated with several impurities. Thus rigorous purification methods are used for purification of leach liquors for obtaining high purity cathode nickel. However in spite of extensive purification of the leach liquors various impurities present in the raw material enter the electrowinning circuit. These impurities in the electrolytic cell affect the deposition characteristics as well as the kinetics and mechanism of the nickel deposition process resulting in low current efficiency and poor nickel deposit.

Nickel electrodeposition is sensitive to the presence of metallic impurities particularly Cr^{3+} , Al^{3+} , Mg^{2+} , Cu^{2+} , Zn^{2+} and sulfur containing organic compounds in the electrolytic bath [1]. These impurities besides increasing the tendency of pitting also change the characteristics of the nickel deposit. Gogia and Das [2] reported that the deposit characteristics and polarisation behaviour were affected strongly in the presence of Mg^{2+} , Mn^{2+} , Al^{3+} and Zn^{2+} but there was no significant change in the current efficiency (CE) at very low concentrations of these ions during electrodeposition of nickel from acidic nickel sulfate solutions. In a separate study [3] they found that low concentrations of

Co^{2+} , Cu^{2+} , Fe^{2+} and Fe^{3+} also had similar effects on nickel electrodeposition. Higher impurity concentrations e.g. $1000 \text{ mg dm}^{-3} \text{ Co}^{2+}$ and $250 \text{ mg dm}^{-3} \text{ Cu}^{2+}$ resulted in cracked, peeled and black nodular deposits. Tripathy et al. [4] who investigated the effects of Li^+ , Na^+ , K^+ and Mg^{2+} on the electrodeposition of nickel from acidic sulfate baths, found that the impurities when present in the electrolytic baths did not affect the nickel electrodeposition current efficiency and electrode polarisation significantly, but some changes in the morphology of the nickel deposits were seen. Srivastava and Tikoo [5] studied the effect of cations like Co^{2+} , Cd^{2+} and NH_4^+ ions on nickel electrodeposition and obtained crack-free nickel deposits in a current density range of $0.2\text{--}1 \text{ A dm}^{-2}$. Kharlamov et al. [6] investigated the effect of impurities such as Cu^{2+} , Co^{2+} and Cd^{2+} on the electrochemical reduction of nickel and found that these impurities inhibited the Ni reduction process and electrodeposits with better texture were obtained.

Cortesi reported [7] that Pb^{2+} and Cd^{2+} ions affected the quality of the deposited metal. At low current density, these ions caused dark spots, pitting, opacity and fragility to the deposits. Yashina [8] observed a sharp deterioration in the quality of the nickel electrodeposit when the nickel bath was contaminated with Fe^{2+} ion. Zosimovic et al. [9] observed a reduction in current efficiency in the presence of Cr^{3+} and V^{6+}

during electrodeposition of nickel at high current densities. Zhou et al. [10] who studied the effect of Al^{3+} and Cr^{3+} on the physical appearance, surface morphology and CE of nickel electrodeposition from sulfate electrolytes observed a change in the surface morphology, internal stress and polarisation behaviour. The magnitude of the effect increased with the impurity concentration in the bath. Zhang [11] also investigated the effects of Al^{3+} & Cr^{3+} on nickel electrodeposition from sulfate solutions. He found that significant degradation of the current efficiency and deposit morphology occurred when these impurities were present in the bath.

Clear information on the effect of Al^{3+} on nickel electrodeposition CE, cathode polarisation and deposit characteristics including crystal orientations and surface morphology is lacking in the literature. In view of this, the present investigation was carried out to evaluate the effect of Al^{3+} on nickel electrodeposition from sulfate baths containing various additives on stainless steel and nickel substrates. The kinetic parameters for the electron transfer process were also determined.

2. Experimental details

The rectangular electrolytic flow-through cell used in this work was similar to that described previously [12]. Ultrapure water (Millipore Milli Q System) was used for preparing the solutions. The nickel electrolyte of composition NiSO_4 (60 g dm^{-3}), Na_2SO_4 (12 g dm^{-3}) and H_3BO_3 (12 g dm^{-3}) was prepared from analytical grade nickel reagents. Dilute sulfuric acid was used to adjust the electrolyte pH. The Al^{3+} concentration in the electrolytic baths was achieved by adding aliquots of aluminium sulfate from a stock solution of concentration 10 g dm^{-3} . The methods used for electrode preparation, electrolysis and deposit examination were similar to our previous paper [13]. The aluminium content in the nickel electrodeposits was determined by dissolving sections of the nickel deposits in dilute HNO_3 and analysing by Inductively Coupled Plasma (ICP) analysis. The cathodic current efficiency (CE) was calculated by the weight method as reported earlier [14].

The preferred crystal orientations of the electrodeposited nickel and the deposit surface morphology were determined by using standard X-ray diffraction and scanning electron microscopy (SEM) methods as described previously [14]. The experimental set up for polarisation studies were similar to that described earlier [15].

3. Results and discussion

3.1. Cathodic Current efficiency and nickel electrodeposition potential

The CE data for nickel electrodeposition from various nickel sulfate baths containing Al^{3+} in the concentration range $0\text{--}40 \text{ mg dm}^{-3}$ are given in Table 1. When no Al^{3+} is present, the CE is found to be 96%, which is consistent with that reported in our previous work [13]. Increasing Al^{3+} concentration causes a progressive decrease in the CE. A similar decrease in CE was reported by Holm and O'Keefe [16] during electrodeposition of nickel from sulfate baths containing Al^{3+} . Our observation is also consistent with Zhang [11] who observed a significant reduction in the current efficiency of nickel electrodeposition from sulfate solutions in the presence of 40 mg dm^{-3} of Al^{3+} . This is also similar to that reported by Zhou et al. [17] who noted a decrease in CE in presence of Al^{3+} . The decrease in CE may be attributed to the adsorption of Al^{3+} species on the cathode surface, which blocks the active sites of the cathode thereby inhibiting the electrocrystallisation of nickel but enhancing hydrogen evolution.

The presence of Al^{3+} in the investigated range ($2\text{--}40 \text{ mg dm}^{-3}$) in the electrolytic nickel bath did not have a significant effect on the nickel electrodeposition potential (CP) as seen from Table 1.

3.2. Nickel deposit characteristics

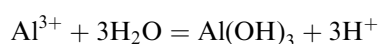
The effect of Al^{3+} in the investigated concentration range ($2\text{--}40 \text{ mg dm}^{-3}$) on the physical characteristics of the nickel deposit is noted in Table 1. It is found that the

Table 1. Effect of Al^{3+} on the CE, cathode potential, aluminium contamination, physical appearance and crystallographic orientations of nickel electrodeposited from acidic sulfate bath

[Al^{3+}] (mg dm^{-3})	CE (%)	CP (V)	Aluminium contamination (%)	Physical appearance	Crystallographic orientations relative peak intensities (I_0/I)			
					(111)	(200)	(220)	(311)
0	96.0	-0.86	—	Smooth, bright, uniform	62	100	—	—
2	95.0	-0.86	0.05	Smooth, bright but less pitted	30	100	2	7
5	94.5	-0.86	0.07	-do-	43	100	35	50
10	93.0	-0.86	0.14	Smooth, bright, deposit with increase in pitting	28	100	5	8
20	91.5	-0.87	0.28	Uniformly cracked and peeled deposit	—	—	—	—
40	89.8	-0.87	0.56	Cracked deposit	—	—	—	—

electrodeposit remains smooth, bright and uniform up to 5 mg dm^{-3} of Al^{3+} . At Al^{3+} concentration higher than 5 mg dm^{-3} pitting in the deposit occurs. This effect increases with increasing Al^{3+} concentration. For example the deposit was cracked and peeled off when 20 mg dm^{-3} Al^{3+} was present.

The nickel electrodeposits obtained in the presence of various Al^{3+} concentrations were analysed for their aluminium content. The results are listed in Table 1. The aluminium content increased with increase in Al^{3+} concentration in the bath. For example, the nickel deposit obtained from the bath containing 2 mg dm^{-3} Al^{3+} has 0.05% Al. The aluminium content was 0.56% when the bath contained 40 mg dm^{-3} . This observation may be attributed to the adsorption of Al^{3+} species on the electrode surface as hydroxides due to surface pH effects during nickel electrowinning [18]. The surface pH of the metal deposit is always higher than the bulk pH when nickel is being deposited. At a higher surface pH the hydrolysis of aluminium ions will be promoted to form aluminium hydroxide precipitates on the nickel deposit thus contaminating it with aluminium.



3.3. Deposit morphology and crystallographic orientations

The data on the effect of Al^{3+} in the concentration range $2\text{--}10 \text{ mg dm}^{-3}$ on the crystallographic orienta-

tions of nickel deposits is also noted in Table 1. The SE micrographs of the nickel deposits are shown in Figure 1. The nickel deposit formed from baths free of Al^{3+} consists of sharp edged crystallites of varying sizes from 1 to $10 \mu\text{m}$ which were randomly oriented [19]. The preferred crystal planes of the deposit are in the order (200) (111) (Table 1).

The addition of 2 mg dm^{-3} of Al^{3+} to the nickel electrolyte results in two new crystal planes (311) and (220), the order of preference being (200) (111) (311) (220). This corresponds to a deposit morphology where round edged crystals with poor grain boundaries are scattered throughout as clusters of crystals (Figure 1(b)). The crystal size is also found to decrease in comparison to that of the deposit obtained from the aluminium free bath. Increasing the concentration of Al^{3+} to 5 mg dm^{-3} favours the growth of (111), (220) and (311) planes and changes the order of preferred crystal orientations to (200) (311) (111) (220). The deposit is more compact and a further reduction in the size of the crystals is observed (Figure 1(c)). Gogia and Das [2] had also observed similar compact deposit morphology in the presence of 5 mg dm^{-3} of Al^{3+} during electrowinning of nickel from sulfate solutions.

Further increase in the Al^{3+} concentration to 10 mg dm^{-3} not only changes the order of crystal orientations (Table 1) but also reduces the peak intensities of (111), (220) and (311) planes. The decrease in the peak intensities of the above planes is also reflected in the change in the surface morphology of the nickel deposits (Figure 1(d)). The characterisation of the

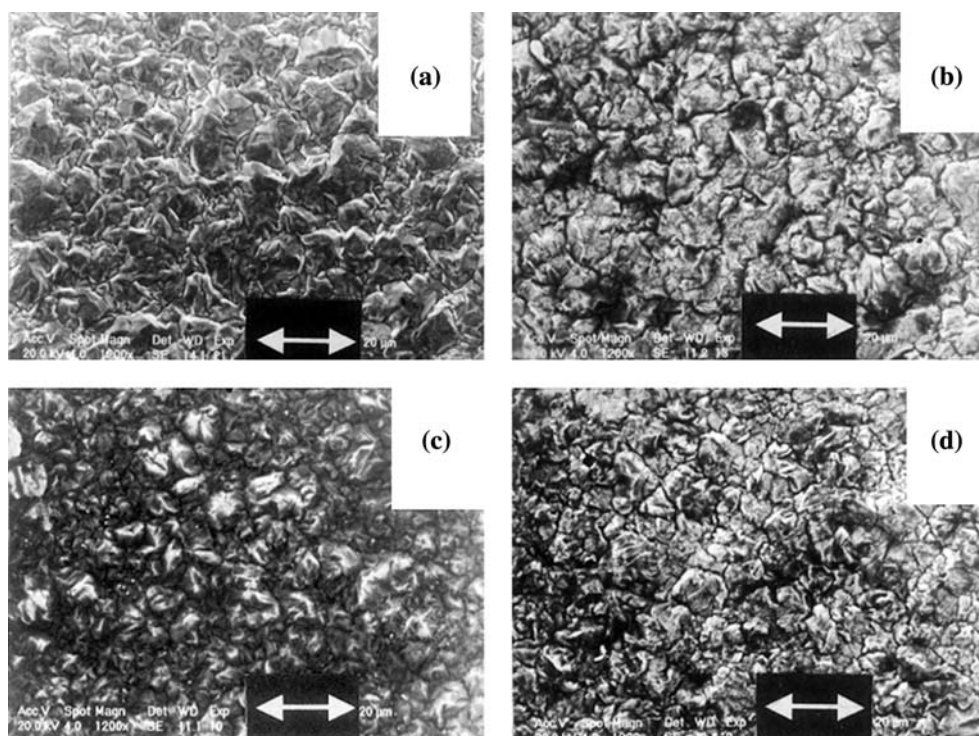


Fig. 1. SE micrographs showing the effect of Al^{3+} on the surface morphology of the nickel electrodeposits (a) $\text{NiSO}_4 + \text{Na}_2\text{SO}_4 + \text{H}_3\text{BO}_3$ (b) a + 2 mg dm^{-3} Al^{3+} (c) a + 5 mg dm^{-3} Al^{3+} (d) a + 10 mg dm^{-3} Al^{3+} . (The dimension bar \leftrightarrow is equivalent to $20 \mu\text{m}$.)

electrodeposits at Al^{3+} concentration higher than 10 mg dm^{-3} was not possible under the present experimental conditions because of poor deposit quality.

3.4. Polarisation studies

The polarisation behaviour of nickel electrodeposition on stainless steel and nickel substrates in the presence of Al^{3+} was investigated using cyclic voltammetry.

Figure 2 shows typical cyclic voltammograms of nickel electrodeposition from various baths i.e. with and without impurities. The cathodic cycle was initiated at 'A' at -100 mV and reversed at 'D' i.e. -950 mV vs SCE. The sharp increase in current at 'C' is ascribed to nickel deposition and the peak at 'F' to nickel dissolution. The shallow peak at 'B' is assigned to hydrogen evolution, which occurs prior to the nickel deposition. This is consistent with the reported literature [20–23]. The nucleation overpotential (NOP) which is the difference between the potential at 'C' and 'E' (the

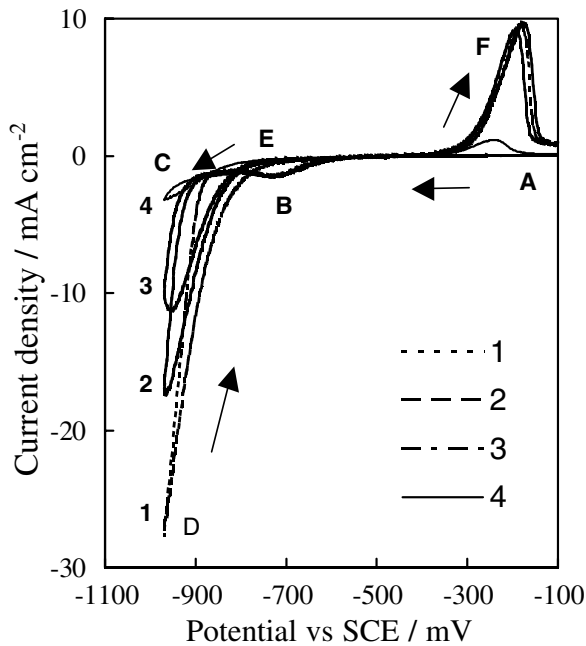


Fig. 2. Cyclic voltammograms showing the polarising effect of Al^{3+} during electrodeposition of nickel from sulfate solutions on stainless steel substrate. Key: (1) Blank (2) 20 mg dm^{-3} (3) 40 mg dm^{-3} (4) 100 mg dm^{-3}

crossoverpotential E_{CO}) [4] was determined from the cyclic voltammogram using the technique similar to that described in our previous paper [14]. The NOP values are recorded in Table 2. The NOP is not much affected when the Al^{3+} concentration is low. However higher concentrations of Al^{3+} ($10\text{--}100 \text{ mg dm}^{-3}$) polarises the cathode significantly and shifts the NOP to more negative values.

The effect of Al^{3+} on cathodic polarisation during nickel electrodeposition on SS and nickel substrate can be seen from the linear sweep voltammograms in Figures 3 and 4, respectively. It can be concluded from these figures that polarisation is higher on stainless steel than on nickel and the presence of Al^{3+} polarises both the electrodes, which increase with increasing Al^{3+} concentration.

The polarisation data were used to calculate the electron transfer kinetic parameters; Tafel slope (b), transfer coefficient (α) and exchange current density (i_0) as described previously [24]. These data are included in Table 2. It is evident that the presence of Al^{3+} has only a marginal effect on the Tafel slope ' b ' when nickel is used as the substrate. As the Al^{3+} concentration changes from 0 to 100 mg dm^{-3} , the ' b ' value remains constant at $125 \pm 3 \text{ mV}$. However the effect of Al^{3+} on

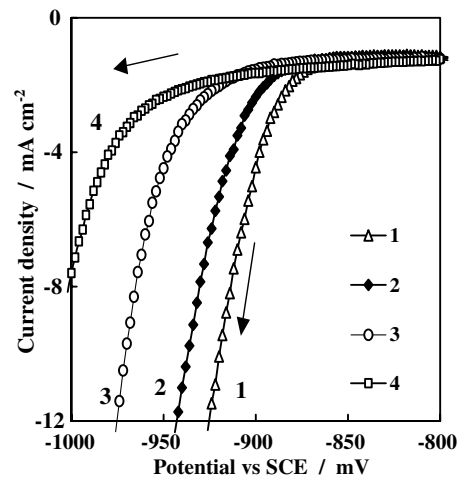


Fig. 3. Linear sweep voltammograms showing the polarising effect of Al^{3+} concentration during nickel electrodeposition on stainless steel substrate. Key: (1) Blank (2) 10 mg dm^{-3} (3) 40 mg dm^{-3} (4) 100 mg dm^{-3}

Table 2. Effect of Al^{3+} on the kinetic parameters b , α and i_0 for nickel electrodeposition from acidic sulfate bath

$[\text{Al}^{3+}]$ (mg dm^{-3})	NOP (mV)	b (mV decade $^{-1}$)		α		i_0 (mA cm^{-2})	
		A	B	A	B	A	B
0	-178	-101	-126	0.59	0.47	6.3×10^{-4}	6.8×10^{-3}
2	-180	-110	-126	0.54	0.47	6.2×10^{-4}	6.4×10^{-3}
5	-182	-110	-128	0.54	0.46	6.0×10^{-4}	6.3×10^{-3}
10	-190	-120	-127	0.49	0.46	5.6×10^{-4}	6.1×10^{-3}
20	-196	-116	-123	0.51	0.48	5.5×10^{-4}	5.9×10^{-3}
40	-202	-123	-122	0.48	0.48	5.2×10^{-4}	5.6×10^{-3}
100	-212	-134	-126	0.49	0.47	4.8×10^{-4}	4.8×10^{-3}

A – Stainless steel; B – Nickel.

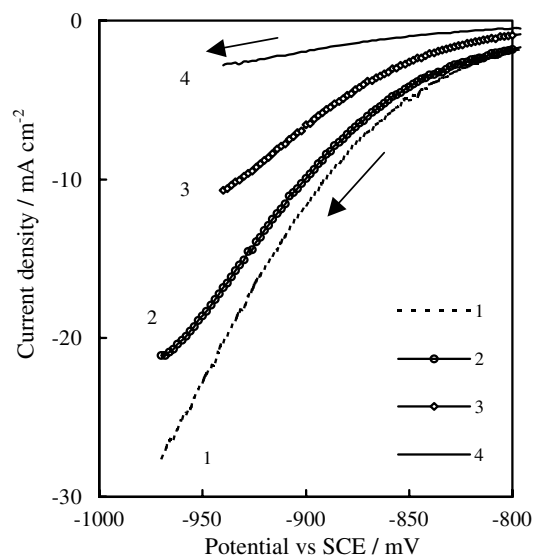


Fig. 4. Linear sweep voltammograms showing the polarising effect of Al^{3+} concentration during nickel electrodeposition on nickel substrate. Key: (1) Blank (2) 10 mg dm^{-3} (3) 40 mg dm^{-3} (4) 100 mg dm^{-3}

'b' values for stainless steel substrate is more significant; 'b' changes from about -100 to $-135 \text{ mV decade}^{-1}$ under similar conditions.

The transfer coefficients for nickel electrodeposition on both nickel and stainless steel remain essentially unaffected in the presence of the investigated concentrations of Al^{3+} . The value of the transfer coefficient remains around 0.5. A similar value of the transfer coefficient for nickel electrodeposition from 1 M nickel chloride solution buffered with boric acid was reported [25]. The i_0 value for nickel electrodeposition on nickel is an order of magnitude higher than on stainless steel substrate irrespective of the presence of Al^{3+} in the bath. We attribute this to the difference in hydrogen overpotential on nickel and stainless steel, being higher for nickel than stainless steel. The effect of presence of Al^{3+} on i_0 values is almost identical for both the substrates i.e. the i_0 values decrease as the Al^{3+} concentration is increased.

4. Conclusions

- (i) The CE of nickel electrodeposition from acidic sulphate baths is not affected by the presence of low concentration of Al^{3+} ($\leq 10 \text{ mg dm}^{-3}$). However, the CE decreases by 5–6% at higher Al^{3+} concentrations.
- (ii) The quality of nickel deposit deteriorates with increasing Al^{3+} concentration in the electrolytic bath.
- (iii) Increase in the Al^{3+} concentration in the bath progressively increases the aluminium content in the nickel deposit.

(iv) The presence of Al^{3+} in the bath not only changes the crystal orientations but also affects the relative growths of various crystal planes. However, the preferred crystal orientation remains unaffected.

(v) Addition of Al^{3+} ($2\text{--}100 \text{ mg dm}^{-3}$) to the electrolytic bath polarises the electroreduction of Ni^{2+} to more negative values.

Acknowledgements

USM would like to thank the CSIR for granting him a research fellowship. The authors thank P. Fallon for assistance in SEM, K. Seymour for XRD and T. B. Issa for general assistance throughout the work. The authors also thank the Director, Regional Research Laboratory, Bhubaneswar, for kind permission to publish this paper. Financial support was partly received from the A.J. Parker Cooperative Research Centre for Hydrometallurgy.

References

1. F.E. Lowenheim, *Modern Electroplating* (John Wiley, 1979), pp. 39–325.
2. S.K. Gogia and S.C. Das, *Met. Trans.* **19B** (1988) 6.
3. S.K. Gogia and S.C. Das, *J. Appl. Electrochem.* **21** (1991) 64.
4. B.C. Tripathy, S.C. Das, P. Singh, G.T. Hefter and D.M. Muir, *J. Appl. Electrochem.* **31** (2001) 581.
5. H.K. Srivastava and P.K. Tikoo, *Plat. Surf. Finish.* **74**(2) (1987) 67.
6. V.I. Kharlmov, A.B. Vakka, T.I. Azarchenko and T.A. Vagramyan, *Elektrokhimiya* **27**(1) (1991) 107.
7. C. Cortesi, *Galvanotech. Processi Plasma* **38**(12) (1987) 303.
8. G.M. Yashina, Z.S. Martenyanova, V.F. Lazarev and N.G. Rossina, *Zash. Met.* **28**(2) (1992) 323.
9. D.P. Zosimovic, N.S. Yurov and V.G. Yurova, *Ukr Khim Zh. Russ (ed)*, **43**(7) (1977) 682.
10. Z. Zhou, M. Holm and T.J. O' Keefe, *Bull. Of Electrochem.* **16**(8) (2000) 358.
11. Z. Zhang (University of Missouri-Rolla, Rolla, Mo, 1997) Ph.D. Dissertation.
12. B.C. Tripathy, P. Singh and D.M. Muir, *Met. Trans.* **32B** (2001) 395.
13. U.S. Mohanty, B.C. Tripathy, P. Singh and S.C. Das, *Minerals Eng.* **15** (2002) 531.
14. U.S. Mohanty, B.C. Tripathy, P. Singh and S.C. Das, *J. Appl. Electrochem.* **31** (2001) 579.
15. U.S. Mohanty, B.C. Tripathy, P. Singh and S.C. Das, *J. Appl. Electrochem.* **31** (2001) 969.
16. M. Holm and T.J. O' Keefe, *Met. Trans.* **31** (2000) 1203.
17. Z. Zhou, M. Holm and T.J. O' Keefe, *Proc. Nickel. Cobalt 97* (1997) Sudbury, Canada, CIM..
18. J. Ji, W.C. Cooper, D.B. Dreisinger and E. Peters, *J. Appl. Electrochem.* **25** (1995) 642.
19. U.S. Mohanty, B.C. Tripathy, P. Singh and S.C. Das, *J. Electroanal. Chem.* **526** (2002) 63.
20. R.K. Dorsch, *J. Electroanal. Chem.* **21** (1969) 495.
21. M. Fleischmann and A.S. Reintjes, *Electrochim. Acta* **29**(1) (1984) 69.
22. J. Horkans, *J. Electrochem. Soc.* **126** (1979) 1861.
23. M. Pushpavanam and K. Balakrishnan, *J. Appl. Electrochem.* **26** (1996) 283.
24. B.C. Tripathy, S.C. Das, G.T. Hefter and P. Singh, *J. Appl. Electrochem.* **29** (1999) 1229.
25. V. Yuza and L. Kopyl, *J. Phys. Chem. (USSR)* **14** (1940) 1071.